GEOPHYSICS, VOL. 60, NO. 6 (NOVEMBER-DECEMBER 1995); P. 1906-1916, 7 FIGS.

Frequency-time decomposition of seismic data using wavelet-based methods

Avijit Chakraborty* and David Okaya*

ABSTRACT

Spectral analysis is an important signal processing tool for seismic data. The transformation of a seismogram into the frequency domain is the basis for a significant number of processing algorithms and interpretive methods. However, for seismograms whose frequency content vary with time, a simple 1-D (Fourier) frequency transformation is not sufficient. Improved spectral decomposition in frequency-time (FT) space is provided by the sliding window (short time) Fourier transform, although this method suffers from the time-frequency resolution limitation. Recently developed transforms based on the new mathematical field of wavelet analysis bypass this resolution limitation and offer superior spectral decomposition. The continuous wavelet transform with its scale-translation plane is conceptually best understood when contrasted to a short time Fourier transform. The discrete wavelet transform and matching pursuit algorithm are alternative wavelet transforms that map a seismogram into FT space. Decomposition into FT space of synthetic and calibrated explosive-source seismic data suggest that the matching pursuit algorithm provides excellent spectral localization, and reflections, direct and surface waves, and artifact energy are clearly identifiable. Wavelet-based transformations offer new opportunities for improved processing algorithms and spectral interpretation methods.

INTRODUCTION

The frequency-domain representation of a time series often illustrates many features that are difficult to visualize in the time domain. The manner in which the time series is mapped into the frequency domain determines the amount of new information that can be obtained. The amplitude and phase spectra of a whole seismogram represent the frequency behavior averaged over the entire (stationary) time series. This standard Fourier-based approach (Claerbout, 1976; Bracewell, 1986; Sheriff and Geldhart, 1983) is a tool for interpretation (Anstey, 1977) and is the basis for seismic data processing methods such as frequency filtering (Claerbout, 1976; Yilmaz, 1987), deconvolution (Lackoff and LeBlanc, 1975; Webster, 1978; Arya and Aggarwal, 1982; Robinson, 1984), and wavelet characteristics (Walden, 1990; Rosa and Ulrych, 1991). Alternatively, instantaneous frequency and phase are attributes of complex trace analysis that are used to describe changes in spectral behavior along the seismogram (Neidell and Poggiagliolmi, 1977; Taner and Sheriff, 1977; Taner et al., 1979; Robertson and Nogami, 1984; Barnes, 1991). However, these attributes are scalar parameters and do not describe the complete spectrum at each time point.

Seismograms whose spectral content vary significantly with time are considered nonstationary and require nonstandard methods of decomposition. One-dimensional time-variant, band-pass filtering based on recursive or Hilbert transform methods are described in Nikolic (1975), Stein and Bartley (1983), and Scheuer and Oldenburg (1988). A more complete description of the time-variant frequency content requires a decomposition into the 2-D frequency-time space. In such a decomposition, the full spectral bandwidth is described for each time and can be used to distinguish between different types of superimposed seismic events. In the short time Fourier transform (STFT) whose history is summarized in Nawab and Quatieri (1988), moving windows of the time domain signal are used to compute their Fourier spectra. Thus this transform maps a 1-D signal into a 2-D frequency-time (FT) plane. Events such as low-frequency surface waves and higher frequency reflections separate in the F-T plane. For example, Okaya et al. (1992) decompose uncorrelated vibroseis data to identify sweep fundamental and harmonic arrivals and also energy that produces correlation artifacts. Because of the invertibility of the STFT, Okaya et al. were able to suppress the artifact energy by selective muting in the FT domain. The STFT, however, has

Manuscript received by the Editor June 13, 1994; revised manuscript received February 6, 1995.
*Dept. of Earth Sciences, University of Southern California, CA 90089.

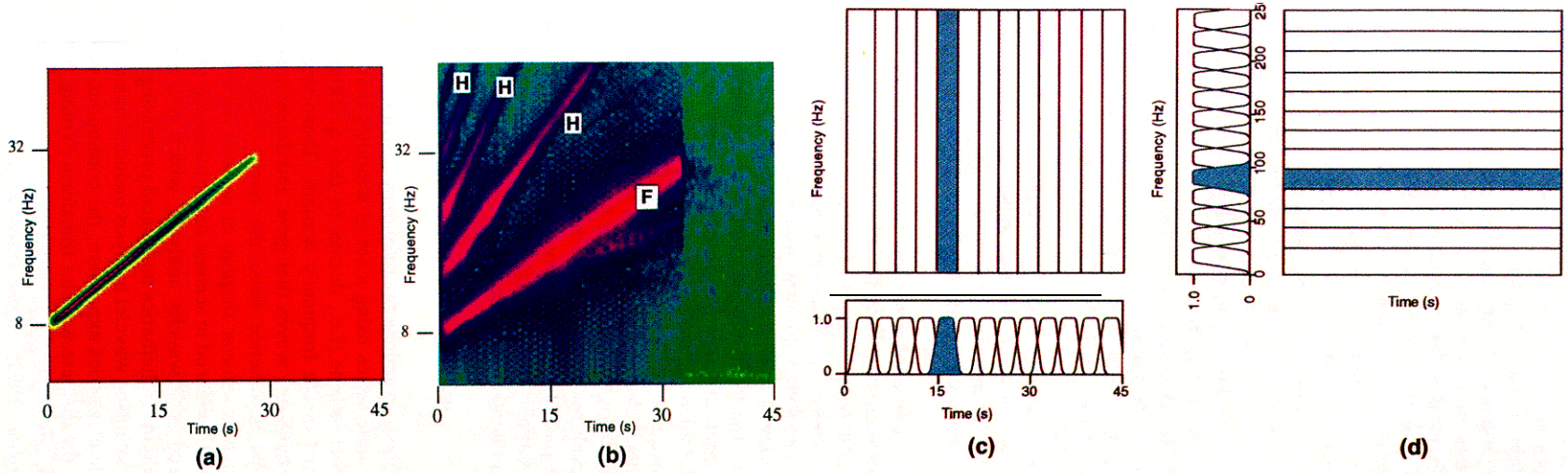

FIG. 1. The short time Fourier transform. (a) STFT of a vibroseis source sweep. (b) STFT of an uncorrelated data trace; note the first arrival and its harmonics (labeled as F and H, respectively). (c) Schematic diagram illustrating the sampling of the FT plane using time domain windows. (d) Schematic diagram illustrating the sampling of the FT plane using frequency-domain windows.

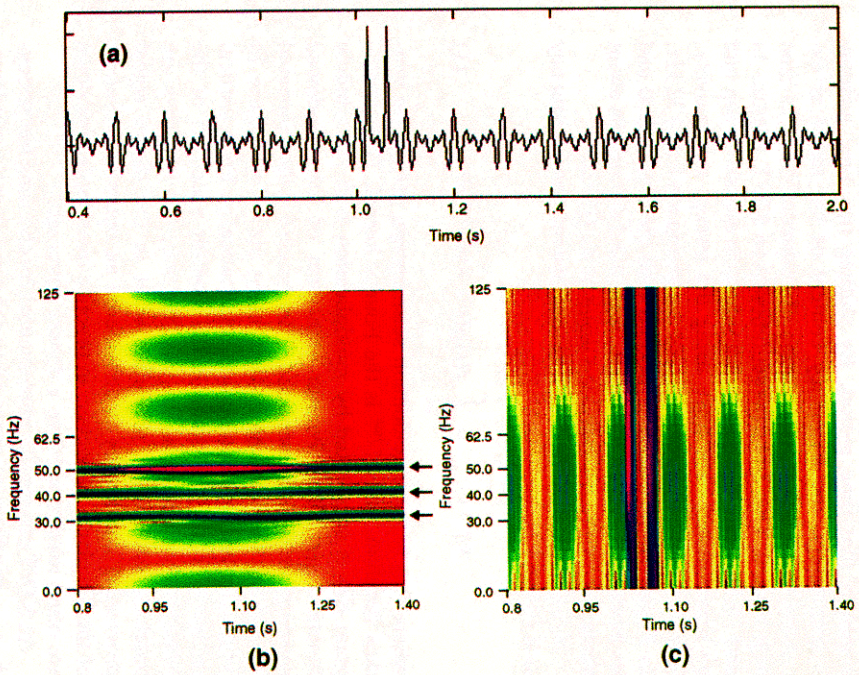

Fig. 2. (a) The time-domain representation of a synthetic signal. (b) An STFT with a long time window. The three cosine waves but not the spikes are well resolved. (c) An STFT with a narrow time window. The spikes are properly localized but the cosine waves are not.

poor time-frequency localization and suffers from the time-bandwidth resolution limitation. Detailed interpretation of the spectral behavior of individual reflections is thus difficult.

A wavelet transform (WT) is an alternative technique to decompose a signal to identify its frequency distribution through time. This technique differs from the STFT in that while an STFT uses a fixed size time window, a wavelet transform uses a variable window size. The WT has been developed since the late 1980s. A large number of contributions have been made by various researchers in, for example, the fields of 1-D signal analysis (Grossmann et al., 1989), time-scale representation (Flandrin, 1989), filter bank theory (Vetterli and Cormac, 1992), digital image processing-edge detection (Mallat and Zhong, 1992; Mallat and Hwang, 1992), numerical analysis (Coifman, 1989; Press, 1992), and seismic data analysis (Pike, 1994; Saito, 1994). In this paper, we first provide a conceptual description of a WT. We then illustrate the improvement in spectral resolution as compared to traditional Fourier-based methods and then discuss possible seismic applications.

SHORT TIME FOURIER TRANSFORM

For a nonstationary signal such as a seismogram, the frequency content changes with time. The amplitude spectrum of the Fourier transform indicates the presence of different frequencies but does not show temporal distribution of these frequencies. If we assume that the signal through a small window of time is stationary, then its Fourier transform provides us with the frequency content of the signal in that time period. By shifting this time window appropriately, the frequency content of the signal is extracted and a 2-D representation of frequencies versus time is produced. This 2-D representation is an STFT. Figures la and lb illustrate the STFT of a vibroseis source sweep and an uncorrelated data trace using the sweep, respectively. The start and end frequencies of the sweep are 8 and 32 Hz. In Figure lb the sweep associated with the first arrival and its harmonics can be identified. A detailed discussion about these events are provided in Okaya et al. (1992).

Mathematically, the STFT at time instant τ and frequency ω is defined as

$$STFT_{(\tau,\omega)} = \int f(t)g(t - \tau)e^{-j\omega t}\, dt, \qquad (1)$$

where *f(t)* is the time-domain seismogram, *g(t)* is the window function, and $e^{-j\omega t}$ is the Fourier kernel. The seismogram *f(t)* is segmented by multiplication with the window function *g(t)*. The Fourier transform of this windowed seismogram is then computed. This process is then repeated by shifting the window in time using $g(t - \tau)$. Figure lc illustrates this implementation schematically. Each vertical rectangle in the FT plane is the Fourier spectrum of the windowed seismogram. In this diagram, the windows are touching each other providing what in the digital signal processing community is considered an optimum coverage of the FT plane. However, in practice overlapping windows are often used to achieve a denser coverage.

An STFT can also be implemented by choosing frequency-domain windows as opposed to the time domain windows. Instead of sampling the time axis with moving windows, the frequency axis can be sampled by a set of fixed bandwidth band-pass filters whose center frequencies are distributed uniformly along the frequency axis (Figure 1d). Each horizontal rectangle in the FT plane is a band-pass filtered version of the original seismogram. The frequency response of the band-pass filters are shown on the left in Figure 1d.

The analysis window function plays an important role in the STFT. If this function has a long duration in time, it becomes a narrow bandwidth band-pass filter in the frequency domain; this implies a fine sampling of the frequency axis. Any subtle variations in the frequency content of the signal will be well resolved in the resulting 2-D STFT plot. However, because of the long time duration, small changes in the time domain become obscured because of averaging. Figure 2a illustrates this behavior by using a synthetic signal that is produced by adding three cosine waves of frequencies 30, 40, and 50 Hz. Two spikes are present at approximately 1 s. Figure 2b illustrates an STFT of this synthetic signal. Because a long time window is used, the three sinusoids are well resolved (arrows in Figure 2b). The individual spikes, however, are not well resolved as the length of the time window is wider than the spacing between the spikes. An averaged representation of the two spikes is present centered at 1 s. The reason for the banded appearance of the spectra of the two spikes is more fully developed in Okaya *(1995).*

The opposite is true for a window function of short time duration that defines short-lived variations in time but fails to detect rapid frequency changes. Figure 2c represents the STFT of the above signal using a narrow time-domain window. The two spikes are now well resolved. However, the three previously well-localized sinusoids have disappeared because the frequency bandwidth of the window is wide and all three different frequencies are now averaged together. This tradeoff is called the uncertainty principle or Heisenberg inequality (Claerbout, 1976). Once a window function has been chosen for an STFT, the time-frequency resolution is fixed over the entire time-frequency plain.

Recently developed techniques such as the wavelet transform, wavelet packet decomposition, and matching pursuit algorithm use variable-width windows and thus do not suffer from resolution limitations of the STFT.

WAVELET ANALYSIS

Wavelet analysis examines the frequency distribution of a nonstationary time series using a set of windows that have compact support in time (i.e., decays to zero quickly) and are band-limited in the frequency domain. These window functions resemble tiny waves that grow and decay in short periods of time and hence have the name "wavelets." Techniques such as *wavelet shaping* or *wavelet deconvolution* that are routinely used in seismic data processing should not be confused with wavelet analysis, which is a newly established field in mathematics and signal processing. Similar to Fourier analysis, wavelet analysis includes transforms such as the wavelet series expansion, the continuous wavelet transform, the discrete wavelet transform (Young, 1993;. Shensa, 1992), and the wavelet packet transform (Coifman and Wickerhauser, 1992). These transforms are invertible

and thus suitable for filtering data. Wavelet analysis acts like a mathematical microscope (Hunt et al., 1993). When the window function has a broad time domain width, a gross picture of the signal structure under consideration is obtained. As the scale changes when the analysis window becomes narrow, the detailed properties of the signal become enhanced.

The continuous wavelet transform was first introduced in Morlet et al. (1982) and Goupillaud et al. (1985), but received full attention of the signal processing community when Daubechies (1988) and Mallat (1989) established connections of the WT to discrete signal processing. Different approaches are taken to implement the continuous wavelet transform and the discrete wavelet transform, as we will discuss next.

THE CONTINUOUS WAVELET TRANSFORM

In a continuous wavelet transform (CWT), the bandwidth of the moving band-pass filter (Le., the frequency-domain window) broadens as the filter center frequency increases. A CWT of a real signal f(t) with respect to an analyzing wavelet $\psi(t)$ is defined as a set of convolutions:

$$W_{(a,b)} = \frac{1}{\sqrt{a}} \int \psi^* \left(\frac{t-b}{a} \right) f(t)\, dt. \qquad (2)$$

The window function $\psi(t)$ is called the kernel wavelet. The parameters *a* and b are called scale and translation, respectively. At each scale (i.e., for each value of *a)* the kernel wavelet is scaled by a factor *1/a* and translated by b to produce the wavelet coefficients $W_{(a\ b)}$. In implementation, *a* is replaced by 2^j, where j is the' scale index. Figure 3 represents a 2-D scale index-translation plot produced by plotting CWT coefficients of the synthetic signal shown in Figure 2a. The frequency response of the window function is plotted on the left in Figure 3. At low scale index, the bandwidth of the window function is narrow. As a result the three sinusoids are well resolved. However the two spikes cannot be identified in the low-frequency region. As the scale index increases, the bandwidth of the window function increases and the time-domain width becomes narrow, thus the two spikes become well resolved.

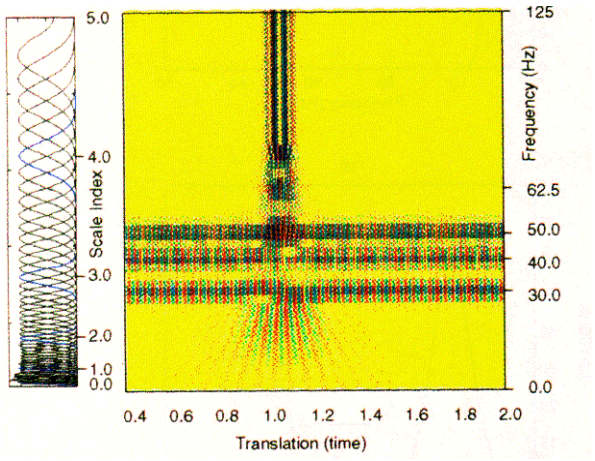

FIG. 3. The continuous wavelet transform of the synthetic signal illustrated in Figure 2a. Scale index is a measure of the octave or harmonic behavior of the center frequency of the frequency-domain filter relative to an original low-band kernel wavelet (filter) function.

If we compare the CWT with the STFT, we observe that both are similar operations. They both decompose a 1-D signal into a 2-D space: (τ, ω) for the STFT and *(a, b)* for CWT, as opposed to a Fourier transform that produces a 1-D spectrum from a 1-D signal. However, the main advantage of using a CWT over a STFT is that the CWT has good frequency resolution for low frequencies and good time resolution for higher frequencies.

Choice of Kernel wavelet

Any function to be used as the kernel wavelet needs to meet the following admissibility conditions (Shensa, 1992; Goupillaud et al., 1985):

1) $\psi(t)$ should be absolutely integrable and square integrable (Le., its energy is finite):

$$\int \psi(t)\, \mathrm{dt} < \infty$$

and

$$\int |\psi(t)|^2\, dt < \infty,$$

and

2) $\psi(t)$ is band limited and has zero mean:

$$\int \left| \frac{\hat{\psi}(\omega)}{\omega} \right| d\omega < \infty.$$

One example of $\psi(t)$ is a modulated Gaussian as defined in Morlet et al. (1982) as

$$\psi(t) = e^{j\nu t} e^{-t^2/2}$$

where

$$\nu \geq 5.$$

Figure 4 shows a Morlet wavelet and its frequency spectrum. Note that both $\psi(t)$ and $\hat{\psi}(\omega)$ are localized in time and frequency, respectively.

A vibroseis correlated (Klauder) wavelet meets the above admissibility conditions but is not as desirable as a Morlet wavelet because of inherent ringiness [i.e., see Goupillaud (1976) or Edelmann (1966)]. However, use of a cosine-squared taper on the original pilot sweep in the field will produce a correlation wavelet very similar to a Morlet wavelet (Bernhardt and Peacock, 1976). An uncorrelated linear or nonlinear sweep also meets the above admissibility conditions. However, Baraniuk and Jones (1993) have determined that the use of a chirp signal as a kernel wavelet produces an unusual mapping into the FT plane, and the usefulness of this decomposition for seismic data still needs

to be determined. Minimum phase (explosive source) wavelets may or may not meet the admissibility conditions. A true impulsive source is analogous to a delta function and thus is not bandlimited and does not have zero mean. Minimum phase sources need to be examined numerically on a case-by-case basis.

DISCRETE WAVELET TRANSFORM

The continuous wavelet transform decomposes a function by band-pass filtering the original signal at different bandwidths. In a discrete wavelet transform (DWT), the same transformation into a 2-D scale-translation space is implemented in a different way. Instead of scaling the kernel wavelet followed by convolution, the DWT is implemented by using quadrature mirror filter (QMF) banks (Vaidyanathan, 1993; Vetterli and Cormac, 1992). QMF is a set of two filters, one low pass and one high pass. During a forward transform, the original signal is filtered by a half-band low-pass and a half-band high-pass filter followed by a down sampling by a factor of two. The output of the high-pass filter is the DWT coefficients for that stage (scale or level). The output of the low-pass filter is then filtered again using the two filters mentioned above. This decomposition is continued until the desired level of decomposition is achieved. Thus at each stage of the transform, the low-pass output is examined in further details using the high-pass filter. This is equivalent to a CWT where the scale index of the kernel wavelet changes by integral values.

The QMFs are efficient, fast (NlogN operations required for an N point DWT) and orthogonal. The wavelets used are also orthogonal, thereby ensuring perfect reconstruction. The implementation of the DWT using QMFs and other multirate filter banks are discussed in detail in signal processing literature (Daubechies, 1988; Mallat, 1989; Rioul and Vetterli, 1991; Vaidyanathan, 1993).

MATCHING PURSUIT DECOMPOSITION

Although the wavelet transform has better time-frequency resolution than an STFT, the resolution is not uniform across the entire time-frequency plane. The wavelet transform has good time resolution for high frequencies (and therefore poor frequency resolution) and good frequency resolution for low frequencies. To get good frequency resolution at intermediate to high frequencies, a wavelet transform alone is not sufficient.

Seismic data are band-limited typically within ranges from 10-15 Hz to 60-70 Hz. This implies that seismograms are rich in intermediate frequencies. As a result, a time-frequency transform capable of producing high resolution for all intermediate frequencies is required for processing seismic data.

Recently two different types of transform techniques have been developed that meet the above mentioned requirements. They are known as wavelet packet decomposition (Coifman and Wickerhauser, 1992) and matching pursuit decomposition (Mallat and Zhang, 1993). Among the two,

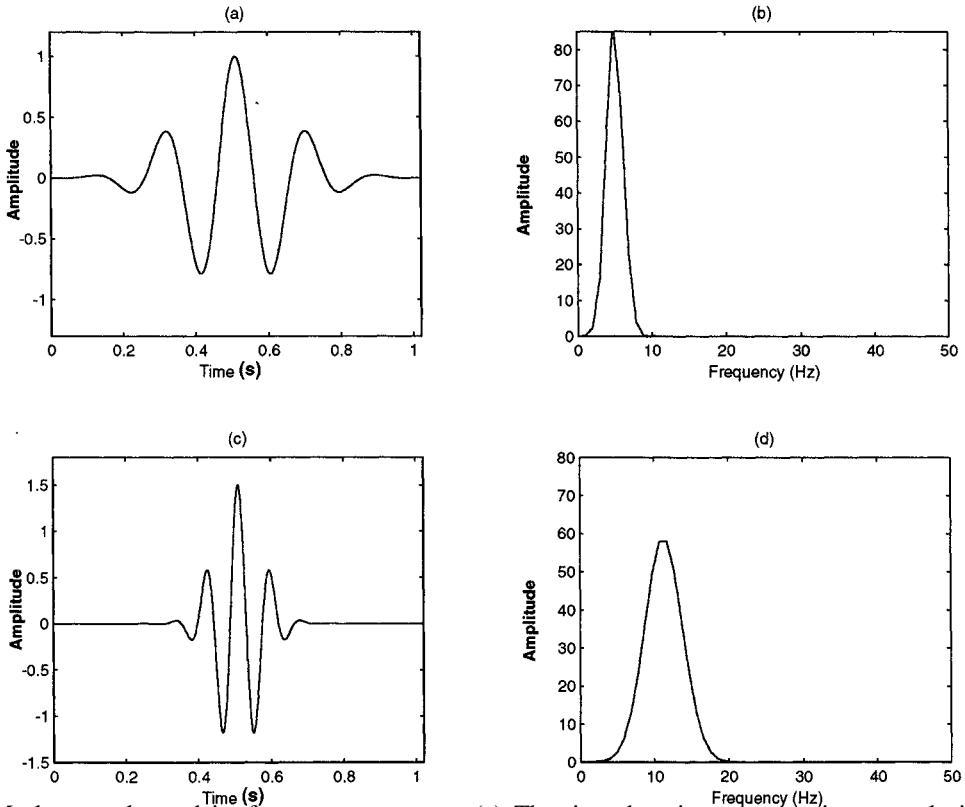

FIG. 4. Morlet wavelet and its frequency spectrum. (a) The time-domain representation at scale index 0. (b) The corresponding frequency spectrum. (c) The time domain representation at scale index 2, and (d) its frequency spectrum.

matching pursuit decomposition provides better resolution (Mallat and Zhang, 1993). We used this algorithm in the present work.

In the matching pursuit decomposition (MPD), a set of basis functions are generated by scaling, translating, and modulating a single window function as:

$$\psi_{(s,\xi,\tau)}(t) = \frac{1}{\sqrt{s}}\psi\left(\frac{t-\tau}{s}\right)e^{i\xi t},$$

where s is the scale, τ is the translation, and ξ is the frequency modulation. The basis functions are called "time-frequency" atoms. If $\psi(t)$ is Gaussian then $\psi_{(s,\xi,\tau)}$ (t) are called Gabor atoms. As shown by Mallat and Zhang (1993), Gabor atoms provide excellent time-frequency resolution. These basis functions or atoms have combinations of all possible time and frequency widths and as a result constitute a redundant set. Once atoms are defined, a best match between the signal and these atoms is found by projecting the atoms onto the signal and then computing the maximum. A residue is then computed by subtracting from the original signal the product of the atoms and the cross product of the selected atom and the signal. This decomposition is continued until the energy of the residue falls below some threshold. This algorithm is discussed in Mallat and Zhang (1993).

COMPARISON OF THE STFT, THE CWT, AND THE MPD

We use a synthetic seismic signal to study the localization properties of the STFT, CWT, and MPD methods. Figure 5a is a synthetic trace produced by the convolution of Ricker wavelets of different center frequencies with a reflectivity series. The reflectivity series has a positive spike at 0.2 s (A), set of three (positive-negative-positive) spikes at 0.5 s (B), a pair of (plus-minus) spikes at 1.0 s (C), and a single spike at 1.6 s (D). FT decompositions of this trace using an STFT, a CWT, and an MPD are plotted in Figures 5b through 5d, respectively.

Reflection A is created using a 40-Hz Ricker wavelet. The STFT of this reflection produced a rectangular region centered at 40 Hz and 0.2 s. Although this indicates the frequency distribution of this reflection, information about the time-location of this event is obscured. The same event can also be identified as the unusual pattern in the CWT plot of Figure 5c, centered at the scale index 3.0 which corresponds to the center frequency of 40 Hz. The CWT failed to provide a good time resolution because the event does not have any high-frequency component. However, this reflection is well resolved both in time and frequency in the FT energy plot of Figure 5d, produced by the MPD.

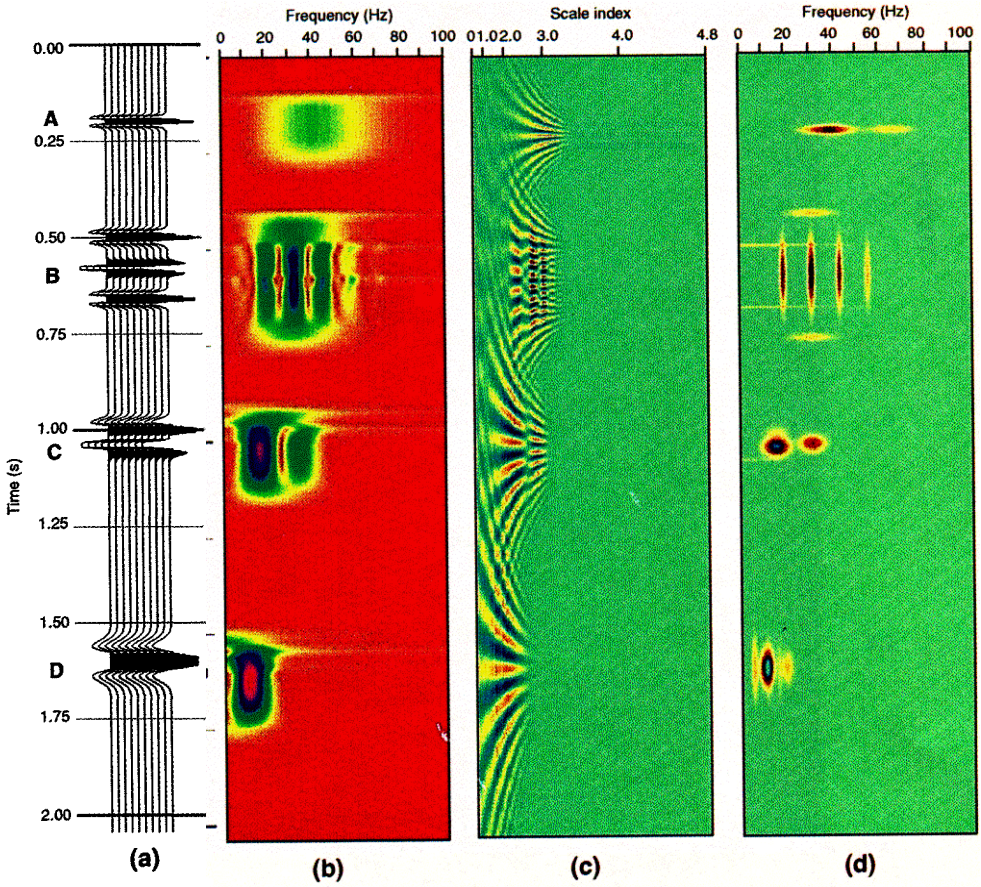

FIG. 5. (a) A synthetic seismogram used in the comparison study of the STFT, the CWT, and the MPD. (b) An FT decomposition produced by an STFT. (c) A scale index-translation plot produced by the CWT. (d) An FT energy distribution produced by the MPD. A decrease in frequency content is observed in all three plots.

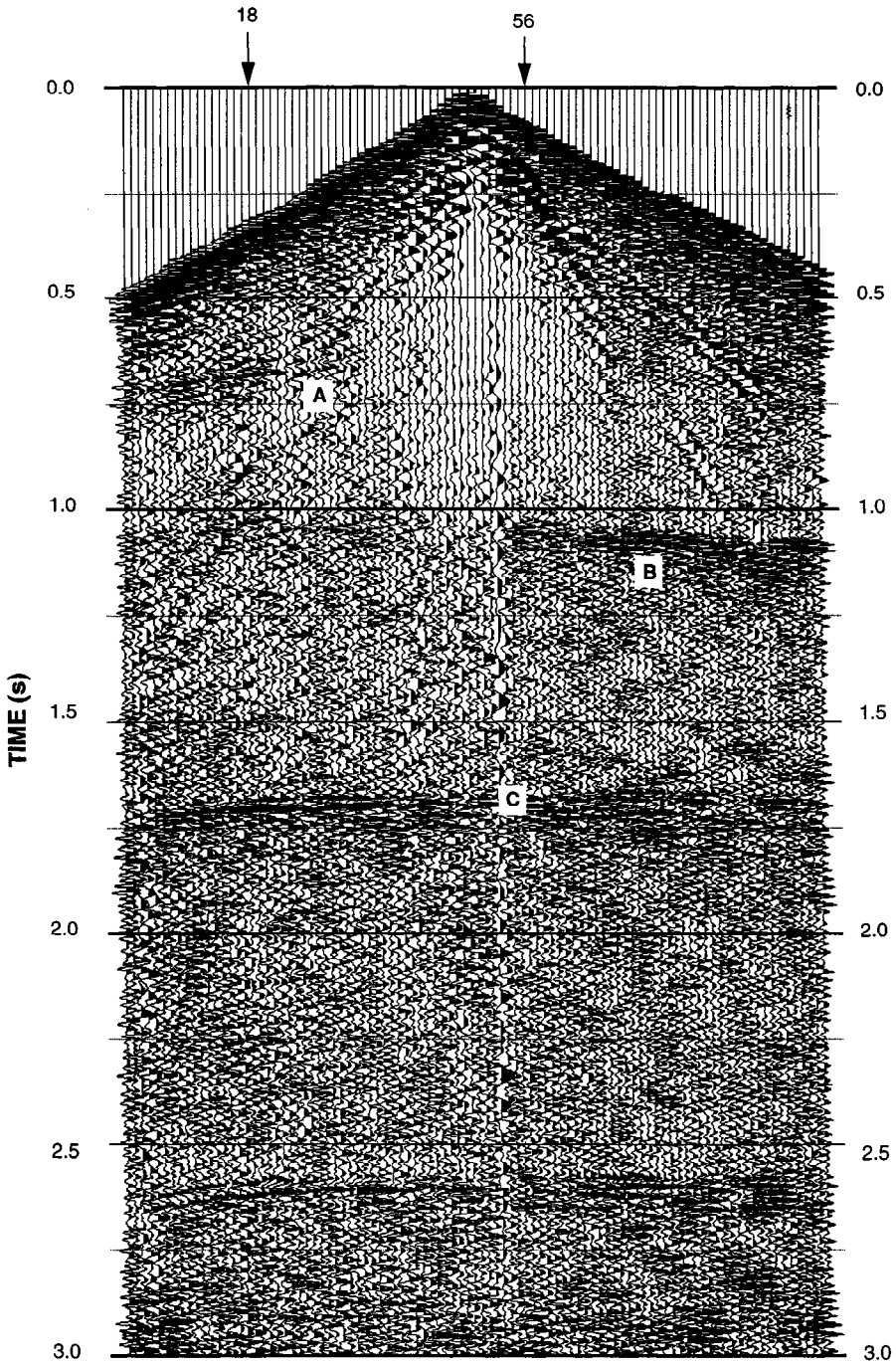

FIG. 6. Shot gather 19, Siljan Sweden. Reflections A, B, C are caused by dolerite sills of 60 m, layered 30 m, and 20 m, respectively. Spectral analyses of traces 18 and 56 are shown in Figure 7.

Event B at 0.5 s is composed of three individual reflections, mimicking a thin layered sequence. A 30-Hz Ricker wavelet is used as the source. The Fourier spectrum of three closely spaced reflections shows banding that is related to the separation of the individual spikes (Okaya, 1995). These bandings can be observed in all three FT plots. However, they are well resolved by the MPD but not the STFT and the CWT. In addition to the banding, two horizontal streaks are present in Figure 5d, indicating the presence of the top and the bottom reflector.

The third event C is composed of two individual reflections. The source is a 20-Hz Ricker wavelet. The top event can be identified in all three plots but with better accuracy in Figure 5d. Information about the top and bottom reflecting spikes is contained in the two different frequency energies (Okaya, 1995). The same observation holds for event D which is a single spike convolved with a 10-Hz Ricker wavelet. Overall frequency content decreases with travel-time as is observed in all three FT plots. Comparing these three methods, it can be concluded that MPD provides the best localization in both time and frequency. In the next section, we use the MPD to decompose seismic traces into their time-frequency components.

INTERPRETATION OF AN F-T DECOMPOSITION USING THE MPD

Figure 6 is a shot gather from Siljan, Sweden (Juhlin, 1988). Several major reflections can be identified. A 6300 m borehole penetrated three of these reflections (A, B, and C); well logs indicate these reflections to be caused by dolerite sills of 60 m, a layered 30 m, and 20 m thicknesses (Juhlin, 1988). The seismic data were collected with a 2 ms sampling rate, producing a Nyquist frequency of 250 Hz.

Figures 7a and 7b illustrate the FT energy distribution of trace 18 and 56 produced using the MPD. Four different types of atoms can be identified. The first is elliptical and elongated in the frequency direction, representing events that are localized in time but possess different frequencies. Reflection events fall in this category. A second type of elliptical atom is elongated in the time direction and represents events that have long time duration but narrow bandwidth. Low-frequency surface waves often fall in this category. The third type of atom is circular in shape. This represents events that have only one or two frequencies and are present for a very short period of time. The fourth type is a long streak in the time direction. This represents a monotonic frequency such as 60 Hz noise that occurs over a long time duration.

In Figure 7a the first arrival is identified at 0.35 s and has a large spread of frequencies ranging from 25 Hz to approximately 100 Hz. Notice the narrow time localization of this arrival. Reflected event A can be identified at 0.6 s. This event is centered at approximately 50 Hz. Event B can be identified as the elliptical atom at 1.0 s. This event is obscured in the shot gather by other seismic energy such as the surface waves. Reflected event C can be identified at 1.75 s. The other circular atoms are caused by random noise that is present in the data. The vertical streaks are shot-generated noise.

Figure 7b illustrates the FT plot of trace 56 that is located near the source. Notice the high-frequency content of the first arrivals, ranging from 75 to 175 Hz. The low-frequency surface waves can be identified at approximately 0.25 s. The dominant frequency of the surface wave is 20 Hz. Reflection B is represented by the elliptical atom at 1.05 s and 60 Hz. Reflection C can be identified as the elliptical atoms near 1.75s. The overall frequency content decreases with time, as observed from the location of these atoms in the FT plane. The center frequency of the atom representing reflection C is higher than that of trace 18. This observation agrees with the fact that the higher frequencies are attenuated as the source energy propagates to greater depths. The vertical streaks represent the source generated noise, visible in the near offset (Figure 6). Because trace 56 is nearer to the source than trace 18, these source-generated noise atoms are well pronounced in this plot.

DISCUSSION AND CONCLUSIONS

A simple 1-D Fourier-based amplitude or phase spectrum provides only an averaged representation of a whole seismogram without information as to local concentrations of energy. What cannot be determined are the appearance of similar bandwidth events at distinctly different times nor superimposed arrivals of different bandwidth. Complex trace analysis is a method to provide time-varying frequency information. However, the instantaneous frequency or phase is a scalar quantity and represents the dominant portion of the waveform at any given time, but this too is a limited description of the seismogram's spectral behavior.

The mapping of a 1-D seismogram, not into a 1-D amplitude spectrum, but to a 2-D frequency-time plane is a major improvement in spectral characterization. Superimposed events of different bandwidth will separate in FT space, and seismic reflections and surface waves with different arrival times and of finite time duration will segregate. In addition, energy such as 60 Hz noise will localize in frequency but be pervasive through time and thus will appear fundamentally different from seismic events (e.g., Figures 2 and 3). Thus, interpretations and processing such as filtering or event suppression are possible in FT space and may be more useful than when conducted in the 1-D Fourier-based frequency domain.

The STFT is a Fourier-based approach to map a seismogram into the FT plane. The STFT has time-frequency resolution limitations as discussed in prior sections. Another difficulty that decreases its resolving capability is the use of finite-length time-domain moving windows over which the 1-D Fourier transforms are performed. In practice, the windows move along the seismogram with a time increment much smaller than the width of the windows. In doing so, a more resolved FT transform is created by finer *sampling* along the time axis. For example, a 500-ms time window incremented every 500 ms will sample a 6.00 s seismogram with 13 windows (including seismogram start and end effects). Alternatively, the same time window incremented every 50 ms will sample with 121 windows. The FT plane of this latter STFT will have the appearance of a more fully resolved 2-D spectrum. However, this gain in detail is balanced by averaging caused by the smaller window incre-

ment; an event will appear in more adjacent windows since it takes longer for the moving window to pass through the event. The event in FT space may appear broader than its actual time duration. Careful selection of STFT parameters such as window length, increment, and window function (tapering) is needed to create meaningful FT spectra.

The wavelet transform provides improved information on the complete (time-variant) character of the spectral content of a seismogram and avoids the difficulties of the STFT. Although a spectrum in the CWT scale-translation domain requires a different viewpoint to fully understand its contents, the frequency-time domain of the MPD transform is easier to comprehend. The appearance of reflections and other seismic events in the wavelet-based FT plane allows for more detailed analysis of the spectral behavior of these events. A better understanding of how to interpret the shape of Gabor atoms and the perturbations in reflection spectra can be developed with careful calibration of the FT spectra

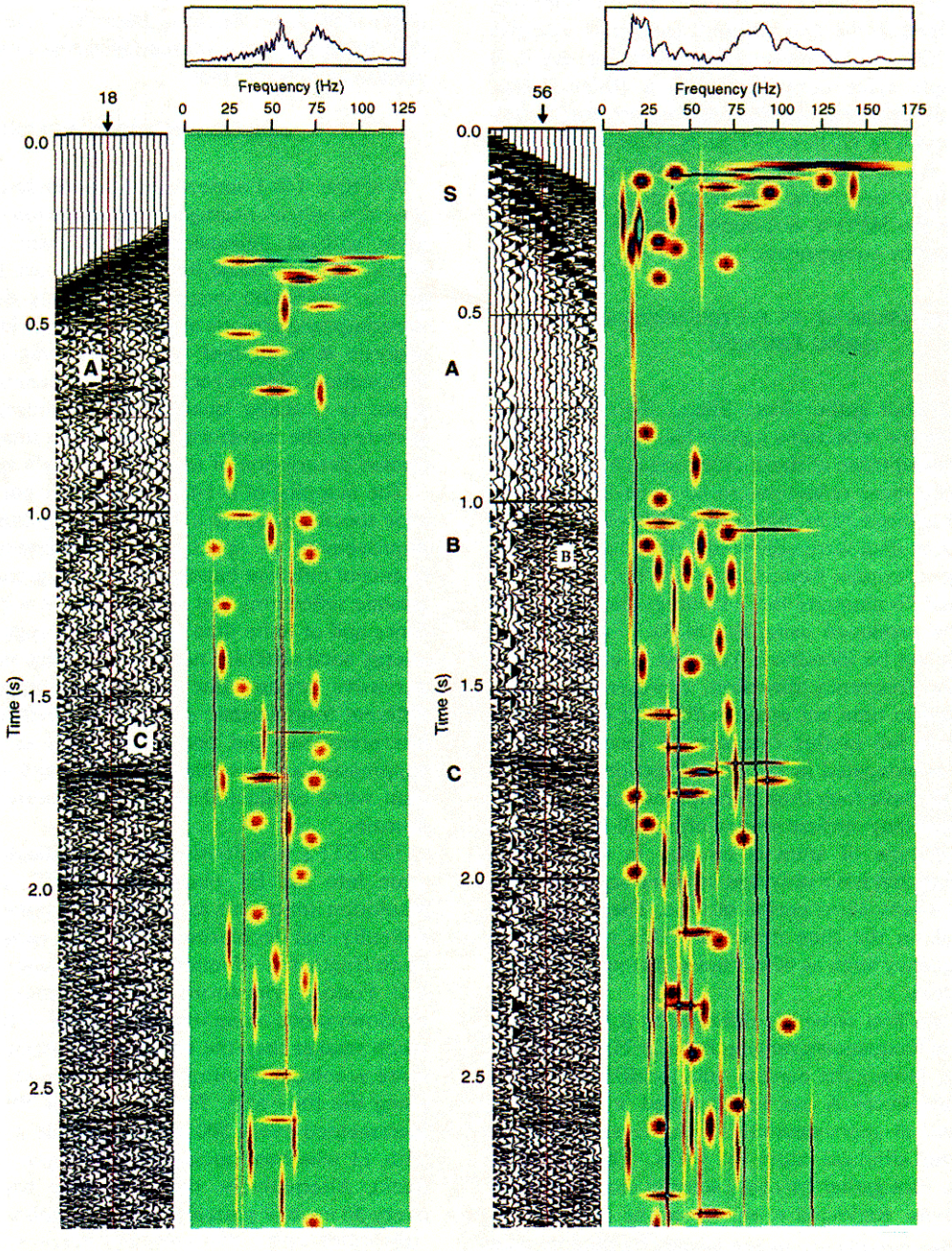

FIG. 7. FT energy distribution of the Siljan data using MPD. (a) Trace 18, and (b) Trace 56. The boxes on top of the FT plots represent the 1-D Fourier spectra of the respective traces.

of reflections with borehole logs and other geologic information as the spectral signatures of a major interface, a thin layer, and a laminated sequence are different (e.g., Okaya, 1995).

The representation of a seismogram's spectral behavior in the FT plane may allow an improved analysis of the attenuation character of the medium through which the seismic energy has propagated. With a more complete 2-D frequency-time spectrum, the loss in energy of any particular frequency can be more completely described. Spectral ratio methods (Sams and Goldberg, 1990) use isolated time windows to compute attenuation values; however, with a 2-D FT spectrum any number of window ratios can be made representing the attenuation between any two traveltimes (depths). In this manner, an inversion for Q structure may be possible by taking advantage of the redundancy offered by analysis of all seismograms for a given CMP point and from one midpoint to another.

The CWT, DWT, and MPD are invertible. While inversion of the CWT depends on the fulfillment of the admissibility conditions as described earlier, exact reconstruction is possible for the DWT (Shensa, 1992) and MPD (Mallat and Zhang, 1993). As a result, wavelet-based methods can be used to filter seismic data. Because of the excellent localization behavior of the MPD, reflections can be enhanced and surface waves and other types of noise can be eliminated using polygonal ("pie-slice") filters in the 2-D FT plane. Because each seismogram is mapped into two dimensions, and thus a shot or CMP gather into three dimensions, filtering algorithms need to be constructed to efficiently handle large volumes of data. Similar filtering can also be applied to CMP stacked traces to improve stack image quality.

Spectral balancing is another process where wavelet methods can be successfully used. An initial estimate of a seismogram's or seismic wavelet's spectral content can be made from the CWT FT plot. The frequency response of the basis wavelets of a CWT cover the frequency axis continuously with uniform amplitude (Figure 3). Weighting of the basis wavelets prior to an inverse CWT is the same as enhancing or weighting selected frequencies in the Fourier domain. However, this weighting in the CWT domain allows for more selective enhancement of specific bands of frequencies due to the number of CWT basis wavelets (filter operators).

Although certain types of signal processing applications using wavelet transforms have been established for geophysical data (e.g., data compression of seismic data (Bosman and Reiter, 1993) and segmentation of well logs (Vermeer and Alkemade, 1993), the full value of the wavelet-based FT-plane spectral decomposition of seismograms has yet to be established. The different wavelet transforms provide spectral information at a level of detail not available with Fourier-based methods and offers new domains for processing and interpreting seismic reflection data.

ACKNOWLEDGMENTS

The authors would like to thank S. Mallat and Z. Zhang for providing their software program to compute the MPD and for the helpful discussion regarding the implementation details of the MPD. We also thank Chris Juhlin for providing the seismic data from Siljan, Sweden. This study was funded under NSF EAR-9206055.

REFERENCES

Anstey, N. A., 1977, Seismic interpretation: The physical aspects: Intemat. Human Res. Develop. Corp.

Arya, V. IS., and Aggarwal, J., 1982, Deconvolution of seismic data: Benchmark papers in electrical engineering and computer science: volume 24 Hutchinson Ross Publ. Co.

Baraniuk, R., and Jones, D., 1993, Shear madeness: New orthonormal bases and frames using chirp functions: IEEE Trans. Signal Proc., 41, 3543-3549.

Barnes, A., 1991, Instantaneous frequency and implitude at the envelope peak of a constant-phase wavelet: Geophysics, 56, 1058-1060.

Bemhardt, T., and Peacock, J., 1976, Encoding techniques for the vibroseis system: Geophys. Prosp., 26, 184-193.

Bosman, C., and Reiter, E., 1993, Seismic data compression using wavelet transforms: 63rd Ann. Intemat. Mtg., Soc. Expl. Geophys., Expanded Abstracts.

Bracewell, R., 1986, The fourier transform and its applications: McGraw-Hill Publ. Co.

Claerbout, J. F., 1976, Fundamentals of geophysical data processing: Blackwell Scientific Publications.

Coifman, R. R., 1989, Multiresolution analysis in non-homogeneous media, in Combes, J. M., Grossmann, A., and Tchamitchian, P., Eds., Wavelets time-frequency methods and phase space: Springer-Verlag, 259-262.

Coifman, R. R., and Wickerhauser, M. V., 1992, Entropy-based algorithms for best basis selection: IEEE Trans. Inform. Th., 38, 713-719.

Daubechies, I., 1988, Orthonormal bases of compactly supported wavelets: Comm. in Pure Applied Math, 41, 909-996.

Edelmann, H., 1966, New filtering methods with "vibroseis": Geophys. Prosp., 14, 455-469.

Flandrin, P., 1989, Some aspects of nonstationary signal processing with emphasis on time-frequency and time-scale methods, in Combes, J. M., Grossmann, A., and Tchamitchian, P., Eds., Wavelets time-frequency methods and phase space: Springer-Verlag, 68-98.

Goupillaud, P., 1976, Signal design in the "vibroseis" technique: Geophysics, 41, 1291-1304.

Goupillaud, P., Grossmann, A., and Morlet, J., 1985, Cycle octave and related transforms in seismi signal analysis, in Geoexpl.: Elsevier Science Publ. B.V., 23, 85-102.

Grossmann, A., Martinet, R. K., and Morlet, J., 1989, Reading and understanding continuous wavelet transforms, in Combes, J. M., Grossmann, A., and Tchamitchian, P., Eds., Wavelets time-frequency methods and phase space: Springer-Verlag, 2-20.

Hunt, J. C. R., Kevlahan, N., Vassilicos, J., and Farge, M., 1993, Wavelets, fractals and Fourier transforms: Detection and analysis of structure, in Farge, M., Hunt, J. C. R., and Vassilicos, J. C., Eds., Wavelets, fractals, and Fourier transforms: Clarendon Press, 1-38.

Juhlin, C., 1988, Interpretation of the seismic reflectors in the gravberg-1 well, in Boden, A., and Eriksson, K., Eds., Deep drilling in crystalline bedrock: Springer-Verlag, 113-121.

Lackoff, M., and LeBlanc, L., 1975, Frequency-domain seismic deconvolution filtering: J. Acoust. Soc. Am., 57, 151-159.

Mallat, S., and Hwang, W., 1992, Singularity detection and processing with wavelets: IEEE Trans. inform. th., 38, 617-643.

Mallat, S., and Zhang, Z., 1993, Matching pursuit with time frequency dictionaries: IEEE Trans. signal prec., 41, 3397-3415.

Mallat, S., and Zhong, S., 1992, Characterization of signals from multiscale edges: IEEE Trans. Pattern analysis and machine intelligence, 14, 710-732.

Mallat, S., 1989, A theory of multi resolution signal decomposition, the wavelet representation: IEEE Trans. pattern analysis and machine intelligence, 11, 674493.

Morlet, J., Arens, G., Fourgeau, E., and D., G., 1982, Wave propagation and sampling theory: Geophysics, 47, 2, 203-236.

Nawab, S., and Quatieri, T., 1988, Short-time Fourier transform, in Lim, J., and Oppenheim, A., Eds., Advanced topics in signal processing: Prentice Hall Signal Processing Series, 289-337.

Neidell, N., and Poggiagliolmi, E., 1977, Stratigraphic modeling and interpretation-geophysical principles and techniques, in Payton, C., Ed., Seismic stratigraphy-Applications to hydrocarbon exploration: Am. Assoc. Petr. Geol., Memoir 26, 389-416.

Nikolic, Z., 1975, A recursive time-varying band-pass filter: Geophysics, 40, 520-526.

Okaya, D. A., 1995, Spectral properties of the earth's contribution to seismic resolution: Geophysics, 60, 241-251.
Okaya, D., Karageorgi, E., McEvilly, T., and Malin, P., 1992, Removing vibrator-induced correlation artifacts by filtering in frequency-uncorrelated time space: Geophysics, 57, 916-926.
Pike, C., 1994, Analysis of high-resolution marine seismic data using the wavelet transform, in Georgiou, E., and Kumar, P., Eds., Wavelets in geophysics: Academic Press, 183-211.
Press, W., 1992, Numerical recipes for fortran: 2nd. ed: Cambridge Univ. Press.
Rioul, O., and Vetterli, M., 1991, Wavelets and signal processing: IEEE Signal Proc. Magazine, no. 11, 14-38.
Robertson, J., and Nogami, H., 1984, Complex seismic trace analysis of thin beds: Geophysics, 49, 344-352.
Robinson, E., 1984, Seismic inversion and deconvolution: Part A: Classical methods: Geophys. Press.
Rosa, A., and Ulrych, T., 1991, Processing via spectral modeling: Geophysics, 56, 1244-1251.
Saito, N., 1994, Simultaneous noise suppression and signal compression using a library of orthonormal bases and the minimum description length criterion, in Georgiou, E., and Kumar, P., Eds., Wavelets in geophysics: Academic Press, 299-324.
Sams, M., and Goldberg, D., 1990, The validity of q estimates from borehole data using spectral ratios: Geophysics, 55, 97-101.
Scheuer, T., and Oldenburg, D., 1988, Aspects of time-variant filtering: Geophysics, 53, 1399-1409.
Shensa, M. J., 1992, The discrete wavelet transform: wedding the a torous and mallat algorithms: IEEE Trans. Signal Proc., 40, 2464-2482.
Sheriff, R., and Geldhart, L., 1983, Exploration seismology, vol. 1 and 2: Cambridge Univ. Press.
Stein, R., and Bartley, N., 1983, Continuously time-variable recursive digital band-pass filters for seismic signal processing: Geophysics, 48, 702-712.
Taner, M., Koehler, F., and Sheriff, R., 1979, Complex seismic trace analysis: Geophysics, 44, 1041-1063.
Taner, M., and Sheriff, R., 1977, Application of amplitude, frequency, and other attributes to stratigraphic and hydrocarbon determination, *in* Payton, C., Ed., Seismic stratigraphy-Applications to hydrocarbon exploration: Am. Assoc. Petr. Geol., Memoir 26, 389-416.
Vaidyanathan, P., 1993, Multirate systems and filter banks: Prentice Hall.
Vermeer, P., and Alkemade, J., 1993, Multiscale segmentation of well logs, *in* Farge, M., Hunt, J. C. R., and Vassilicos, J. C., Eds., Wavelets, Fractals, and Fourier transforms: Clarendon Press, 143-149.
Vetterli, M., and Cormac, H., 1992, Wavelets and filter banks: Theory and design: IEEE Trans. Signal Proc., 40, 2207-2231.
Walden, A., 1990, Improved low-frequency decay estimation using the multitaper spectral analysis method: Geophys. Prosp., 38, 61-86.
Webster, G., 1978, Deconvolution: Geophysics Reprints, Soc. Expl. Geophys., vol 1.
Yilmaz, O., 1987, Seismic data processing: Soc. Expl. Geophys.
Young, R. K., 1993, Wavelet theory and its applications: Kluwer Academic Publishers.